processes of $[Fe_4S_4Cp_4]$ (and some analogous compounds) are in agreement with the now proposed $n = 0$ to 4+ oxidation states.[12] The new assignments made in the case of $[Fe_4(CO)_4Cp_4]$, however, are not supported by our entropy data.

Apart from the small differences in half-wave potentials for $[Fe_4S_5Cp_4]$ and $[Fe_4S_4Cp_4]$, the main difference in redox behavior is that $[Fe_4S_5Cp_4]$ can be reduced to the 1- and 2- ion. The oxidation to the 4+ ion of $[Fe_4S_5Cp_4]$ is probably outside the potential window of our experiments.

Thus, our results demonstrate that $[Fe_4S_5Cp_4]$ exists at six different oxidation states and that the cluster structure is kept intact during five of these (n = 1- to 3+). This is quite noteworthy, since few species possess this property, and the addition or subtraction of more than one electron usually leads to a structural disruption. So far, $[Fe_4S_4Cp_4]^n$[2,3] and $[Fe_4S_4(SR)_4]^n$ (R = C_6H_5, $C(CH_3)_2CH_2OH$, 2,4,6-(i-Pr)$_3C_6H_2$)[13,14] are the only other tetranuclear Fe clusters known to exist at five and four different oxidation states, respectively. Ferrocene-type compounds, such as 1,1′-quaterferrocene[15] and $(C_{10}H_8)(C_6Me_6)Fe_2^n$ (n = 2+ to 2-),[16] have also been reported to exhibit five oxidation states.

The structural data (by X-ray diffraction[6,7] and/or Fe-EXAFS[17]) for $[Fe_4S_5Cp_4]$ in its neutral, monopositive and dipositive states being available, it was of interest to correlate the observed structural variations in the Fe_4S_5 core with the successive reductions and to predict its geometry in the (as yet) nonisolated mono- and dianions. The major changes encountered are primarily reflected in the Fe–Fe interactions. The averaged Fe–Fe distances, presented in Table II, increase steadily upon reduction (from 2.63 to 2.78 and then to 2.96 Å). A more detailed analysis shows that, from the dication to the monocation and then to the neutral cluster, one of the two bonding Fe–Fe interactions weakens as the bonding length increases from 2.63 to 2.91 and then to 3.31 Å, while the other remains approximately constant (2.61 to 2.65 Å). In other words, the addition of the first and then of the second electron causes the lengthening of one of the Fe–Fe distances until it stretches well beyond the 3-Å limit. If the same trend persists when adding more electrons, one can assume that, after addition of a fifth electron to form $[Fe_4S_5Cp_4]^{2-}$, there will be no Fe–Fe bonding interactions left. This coincides with the breakdown of the Fe_4S_5 core structure, since we observed that $[Fe_4S_5Cp_4]^{2-}$ is unstable and expels sulfur. Metal–metal interactions therefore appear to play an important role in the stability of the $[Fe_4S_5Cp_4]$ series and its capability of "adsorbing" several electrons without undergoing any major structural changes.

Acknowledgment. We thank Professor J. J. Steggerda for his stimulating interest in this work.

(12) Blonk, H. L.; Berkelmans, J. F. J.; van der Linden, J. G. M., in preparation.
(13) Pickett, C. J. *J. Chem. Soc., Chem. Commun.* **1985**, 323.
(14) (a) Mascharak, P. K.; Hagen, K. S.; Spence, J. T.; Holm, R. H. *Inorg. Chim. Acta* **1983**, *80*, 157. (b) O'Sullivan, T.; Miller, M. *J. Am. Chem. Soc.* **1985**, *107*, 4096.
(15) Brown, G. M.; Meyer, T. J.; Cowan, D. E.; LeVanda, C.; Kaufman, F.; Roling, P. V.; Rausch, M. D. *Inorg. Chem.* **1975**, *14*, 506.
(16) Desbois, M. H.; Astruc, D.; Guillin, J.; Mariot, J. P.; Varret, F. *J. Am. Chem. Soc.* **1985**, *107*, 5280.
(17) Diakun, G.; Jordanov, J., submitted for publication.

Contribution from the Dipartimento di Chimica Inorganica e Struttura Molecolare, Università di Messina, 98100 Messina, Italy, and Dipartimento di Chimica, Università di Siena, 53100 Siena, Italy

Synthesis, X-ray Crystal Structure, and Electrochemical Properties of the Rh_2^{4+} Complex $Rh_2(form)_4$ (form = *N,N′*-Di-*p*-tolylformamidinate Anion)

Pasquale Piraino,*† Giuseppe Bruno,† Sandra Lo Schiavo,† Franco Laschi,‡ and Piero Zanello*‡

Received August 5, 1986

The reaction of the dirhodium(II) mixed-ligand complex $Rh_2(form)_2(O_2CCF_3)_2(H_2O)_2$ (form = *N,N′*-di-*p*-tolylformamidinate anion) with free *N,N′*-di-*p*-tolylformamidine (mole ratio 1:4) leads to the formation of the complex $Rh_2(form)_4$ (**1**) in excellent yield. The complex was characterized by a single-crystal X-ray diffraction analysis, crystallizing in the space group $Pn\bar{3}n$, with a = 20.990 (2) Å, V = 9248 Å^3, Z = 6, R = 0.036, and R_w = 0.0378. The Rh–Rh [2.4336 (4) Å] and the Rh–N [2.050 (5) Å] bond distances are well in the range observed for this class of compounds. The molecule is in a staggered conformation, with N–Rh–Rh–N torsion angles of 16.7 (2)°. Complex **1** reacts with carbon monoxide, giving the monocarbonyl adduct $Rh_2(form)_4(CO)$ (**2**), characterized by elemental analysis and IR, ^{13}C NMR, and electrochemical measurements. Unlike other dirhodium(II) carbonyl derivatives, **2** is remarkably stable. In the ^{13}C NMR spectrum a dramatic upfield shift is seen for the carbonyl resonance (δ 144.06); the IR spectrum shows ν(CO) at 2040 cm^{-1}. These data coupled to electrochemical measurements suggest that the π back-bonding is reasonably strong in **2**. The electrode behavior of **1** has been investigated in different nonaqueous solvents. Complex **1** undergoes two anodic redox changes, Rh(II)–Rh(II)/Rh(II)–Rh(III) (reversible) and Rh(II)–Rh(III)/Rh(III)–Rh(III) (irreversible), and one cathodic change, Rh(II)–Rh(II)/Rh(II)–Rh(I) (irreversible), under cyclic voltammetry. The ESR spectrum at 100 K of the species $[Rh_2(form)_4]^+$ displays $g_\perp$ = 2.062 and $g_\parallel$ = 1.957. The $g_\parallel$ is split into a 1:2:1 triplet by two equivalent rhodium nuclei ($A_\parallel = 18.9 \times 10^{-4}$ cm^{-1}). The generated Rh(II)–Rh(III) species is quite stable, and it belongs to the completely delocalized "class III" (Robin–Day) mixed-valent derivatives.

Introduction

The chemistry of the complexes containing the Rh_2^{4+} core, represented by the parent complex $Rh_2(O_2CCH_3)_4$, was dominated until recently by complexes containing four carboxylates as bridging ligands, known as the "lantern" structure.[1] Rh_2^{4+} complexes containing the N–C–O groups, $[Rh_2(mhp)_4$ (mhp = 6-methyl-2-hydroxypyridinato),[2] $Rh_2(RNOCR')_4$ (R = C_6H_5; R′ = CH_3)[3]], the N–C–N groups $[Rh_2(PhNpyr)_4$,[4] $Rh_2(N_2R_2CR)_4$[5]], or the pyrazolate anion[6] $[Rh_2(3,5\text{-}Me_2pz)_4]$ were isolated recently.

For all of the above-mentioned Rh_2^{4+} complexes, the observed chemical reactivity is limited to introduction of an axially coordinated ligand. In some cases,[4] this is prevented by the steric

(1) (a) Felthouse, T. R. *Prog. Inorg. Chem.* **1982**, *20*, 109. (b) Boyer, E. B.; Robinson, S. D. *Coord. Chem. Rev.* **1983**, *50*, 109. (c) Cotton, F. A.; Walton, R. A. *Multiple Bonds between Metal Atoms*; Wiley-Interscience: New York, 1982; p 311.
(2) (a) Berry, M.; Garner, C. D.; Hillier, I. H.; Macdowell, A. A.; Clegg, W. *J. Chem. Soc., Chem. Commun.* **1980**, 494. (b) Cotton, F. A.; Felthouse, T. R. *Inorg. Chem.* **1981**, *20*, 584.
(3) Duncan, J.; Malinski, T.; Zhu, T. P.; Hu, Z. S.; Kadish, K. M. *J. Am. Chem. Soc.* **1982**, *104*, 5507.
(4) Tocher, D. A.; Tocher, J. H. *Inorg. Chim. Acta* **1985**, *104*, L15.
(5) Le, J. C.; Chavan, M. Y.; Chau, L. K.; Bear, J. L.; Kadish, K. M. *J. Am. Chem. Soc.* **1985**, *107*, 7195.
(6) Barron, A. R.; Wilkinson, G.; Motevalli, M.; Hursthouse, M. B. *Polyhedron* **1985**, *4*, 1131.

† Università di Messina.
‡ Università di Siena.

0020-1669/87/1326-2205$01.50/0

hindrance of the coordinated groups. The enhanced electron density within the Rh_2^{4+} core due to better σ-donor ligands causes dramatic effects on the redox properties of such complexes. Kadish and Bear observed that the substitution of the eight oxygen atoms of the coordination sphere of carboxylates with four NH groups not only dramatically favors the electrochemical access to the Rh(II)–Rh(III) species but, in some cases, also makes accessible the Rh(III)–Rh(III) species.[7] While the tetrakis(anilinopyridinato) complex $Rh_2(PhNpyr)_4$[4] and the tetrakis(benzamidinato) complex $Rh_2(N_2Ph_2CPh)_4$[5] effectively display two facile one-electron oxidation steps, the tetrakis(pyrazolato) complex $Rh_2(3,5\text{-}Me_2pz)_4$[6] is irreversibly oxidized at relatively high potentials. Interestingly, the complex containing four benzamidinates as bridging ligands shows a quasi-reversible one-electron reduction attributable to the formation of the Rh(I)–Rh(II) species.[5] The complexes containing the Rh_2^{n+} (n = 3, 6) core were identified only by electrochemical methods and ESR spectroscopy and were never isolated owing to their instability, probably because of further redox processes. Adjustment of the electron density within the Rh_2^{4+} core by means of the appropriate ligands could permit the stabilization of Rh_2^{n+} (n = 3, 6) complexes.

Following our recent work on dirhodium formamidinate complexes,[8,9] we recently reported the synthesis of the dirhodium(II) mixed-ligand complex $Rh_2(form)_2(O_2CCF_3)_2(H_2O)_2$[10] (form = *N,N'*-di-*p*-tolylformamidinate anion). The trifluoroacetate groups are very labile; consequently, this complex has a rich chemistry and has proven to be an ideal starting material for the synthesis of other Rh_2^{4+} complexes. This paper deals with the synthesis, X-ray analysis, and electrochemical studies of the complex $Rh_2(form)_4$ (**1**), obtained by displacement of the trifluoroacetate groups from the above named mixed-ligand complex. We also report the synthesis of the complex $Rh_2(form)_4(CO)$ (**2**), a stable carbonyl adduct.

Experimental Section

Starting Materials. $Rh_2(form)_2(O_2CCF_3)_2(H_2O)_2$ was prepared by the literature procedure.[10] The supporting electrolyte tetrabutylammonium perchlorate, $[NBu_4]ClO_4$ (Fluka), was dried in a vacuum oven at 100 °C and used without further purification (*danger* in use of perchlorates in *general*). The solvents used for electrochemistry [dichloromethane, acetonitrile, tetrahydrofuran, and *N,N*-dimethylformamide (Burdick and Jackson) and pyridine (Aldrich)] were of "distilled in glass" grade and were used as received.

Apparatus. Infrared spectra were recorded on KBr pellets with a Perkin-Elmer 783 instrument. Electronic absorption spectra were run as $CHCl_3$ solution on a Perkin-Elmer Lambda 5 UV-visible spectrophotometer. ^{13}C NMR spectra were recorded on a Bruker WH 400 spectrometer. ESR experiments were performed with a Bruker X-band ER 200D-SRC spectrometer. The external magnetic field was calibrated with a microwave bridge ER 041MR wavemeter, and the temperature was controlled (±1 K) with a Bruker ER 4111 VT variable-temperature unit. Elemental analyses were performed by the Microanalytical Laboratory of the Organic Chemistry Institute of Milan and Analytische Laboratorien Malissa and Reuter, Elbach, West Germany. The electrochemical apparatus has been described elsewhere.[11] Potential values (measured at 20 ± 0.1 °C) are referred to an aqueous saturated calomel reference electrode (SCE). Extra pure nitrogen was employed to remove oxygen from tested solutions.

Synthesis of $Rh_2(form)_4$ (1). A mixture of solid $Rh_2(form)_2(O_2CCF_3)_2(H_2O)_2$ (0.30 g, 0.32 mmol) and *N,N'*-di-*p*-tolylformamidine (0.287 g, 1.28 mmol) (molar ratio 1:4) was heated at 135 °C for 30 min. The green molten mixture obtained was cooled to room temperature and washed repeatedly with 10-mL portions of diethyl ether to remove the unreacted formamidine. Crystallization of the remaining greenish solid from benzene-heptane gave analytically pure material as green plates (83% yield). Anal. Calcd for $Rh_2C_{60}H_{60}N_8$: C, 65.57; H, 5.50; N, 10.19. Found: C, 65.37; H, 5.48; N, 10.25. Infrared spectrum (KBr pellet; cm^{-1}): ν(N–C–N) 1585 (s). Electronic spectrum [$CHCl_3$ solution; λ_{max}, nm (ϵ, M^{-1} cm^{-1})]: 472 (4242), 573 (675). ^{13}C NMR (30 °C, $CDCl_3$): δ 20.72 (s, CH_3). ^1H NMR (30 °C, $CDCl_3$): δ 2.2 (s, CH_3).

Synthesis of $Rh_2(form)_4(CO)$ (2). Complex **1** (0.2 g, 0.18 mmol) was dissolved in CH_2Cl_2 (20 mL), and carbon monoxide was bubbled through the solution for 10 min. The color of the solution, initially yellow-green, turned pink. On addition of hexane and removal of the dichloromethane in vacuo, a pink-red solid was obtained in essentially quantitative amounts. Anal. Calcd for $Rh_2C_{61}H_{60}N_8O$: C, 65.01; H, 5.36; N, 9.84; O, 1.41. Found: C, 65.13; H, 5.35; N, 9.85; O, 1.50. Infrared spectrum (KBr pellet; cm^{-1}): ν(CO) 2040 (s); $\nu(^{13}CO)$ 1996 (s), ν(N–C–N) 1580 (vs). ^{13}C NMR (30 °C, $CDCl_3$): δ 144.06 (dd, $^1J_{Rh-CO}$ = 51, $^2J_{Rh-CO}$ = 24 Hz), 19.82 (s, CH_3), 19.68 (s, CH_3).

X-ray Data Collection and Structure Refinement. Suitable green-yellow crystals of complex **1** of cubic habit were obtained by slow evaporation from a benzene–heptane solution. Data for a crystal of approximate dimensions 0.12 × 0.12 × 0.12 mm were collected on a Siemens-Stoe four-circle diffractometer at room temperature using Mo Kα radiation (λ = 0.71069 Å). Accurate unit-cell dimensions and crystal orientation matrices were obtained from least-squares refinement of 2θ, ω, χ, and ϕ values of 20 reflections in the range $15 < 2\theta < 30°$.

The compound crystallizes in the cubic space group $Pn\bar{3}n$, with a = 20.990 (2) Å, V = 9248.1 Å^3, Z = 6, and D(measd) = 1.30 g cm^{-3}. Lorentz and polarization corrections were applied, but none for absorption (μ = 5.10 cm^{-1}). The structure was solved by using standard Patterson methods, least squares, and the Fourier technique. Of 7943 reflections measured with an ω/θ scan technique in the range $3 \le 2\theta \le 50$, 553 (averaged) having $I > 3\sigma(I)$ were used to refine 87 parameters to final residuals of $R = \sum(|F_o| - |F_c|)/\sum|F_o| = 0.036$ and $R_w = |\sum w(|F_o| - |F_c|)^2/\sum w|F_o|^2|^{1/2} = 0.0378$. The function minimized was $W\Delta^2$ in which $W = 1.6809/(\sigma^2|F_o| + 0.001206F_o^2)$ and $\Delta = |F_o| - |F_c|$. Hydrogen atoms were refined isotropically. The observed density implies that the crystal chosen for data collection contains molecules of solvent in the unit cell. Attempts to locate these molecules were not successful because, as in the case of the isostructural complexes $Ni_2(form)_4$ and $Pd_2(form)_4$,[12] they are highly disordered. Other procedures for data collection and structure refinement have been presented elsewhere.[9] Atomic scattering factors were taken from ref 13; the anomalous scattering of rhodium was from ref 14. All the calculations were performed with the "SHELX 76"[15] set of programs on the IBM 4341 computer of the Centro di Calcolo dell'Università di Messina.

Temperature factors (Table V) and structure factors have been deposited as supplementary material.

Results and Discussion

The green-yellow air-stable complex $Rh_2(form)_4$ dissolves easily in chlorinated solvents, benzene, and tetrahydrofuran and to a lesser extent in acetonitrile; it is insoluble in other coordinating solvents such as acetone or dimethyl sulfoxide.

Infrared and ^1H NMR data spectra of **1**, listed in the Experimental Section, were not of much help in assigning the structure, which was determined by the X-ray analysis.

The complex exhibits only a limited tendency for axial coordination, indicated by the lack of reactivity with PPh_3, methylimidazole, and piperidine. Steric or electronic factors may account for this inertness, but the most likely explanation involves unfavorable steric interactions due to the presence of the four *p*-tolyl groups that do not leave the metal centers open to attack by most Lewis bases. Only ligands with small steric hindrance such as CO can be accommodated into the axial positions.

Another marked divergence in reactivity between complex **1** and the classic rhodium carboxylate derivatives is evidenced by the reaction with carbon monoxide, which gives $Rh_2(form)_4(CO)$ (**2**). Attempts to grow suitably sized crystals of **2** for X-ray analysis were not successful. Complex **2** is remarkably stable for some weeks in the solid form as well as in $CHCl_3$ solution and

(7) (a) Bear, J. L.; Zhu, T. P.; Malinski, T.; Dennis, A. M.; Kadish, K. M. *Inorg. Chem.* **1984**, *23*, 674. (b) Chavan, M. Y.; Zhu, T. P.; Lin, X. Q.; Ahsan, M. Q.; Bear, J. L.; Kadish, K. M. *Inorg. Chem.* **1984**, *23*, 4538. (c) Chakravarty, A. R.; Cotton, F. A.; Tocher, D. A.; Tocher, J. H. *Inorg. Chim. Acta* **1985**, *101*, 185.
(8) Piraino, P.; Tresoldi, G.; Faraone, F. *J. Organomet. Chem.* **1982**, *224*, 305.
(9) Piraino, P.; Bruno, G.; Nicolò, F.; Faraone, F.; Lo Schiavo, S. *Inorg. Chem.* **1985**, *24*, 4760.
(10) Piraino, P.; Bruno, G.; Tresoldi, G.; Lo Schiavo, S.; Zanello, P. *Inorg. Chem.* **1987**, *26*, 91.
(11) Zanello, P.; Leoni, P. *Can. J. Chem.* **1985**, *63*, 922.
(12) Cotton, F. A., personal communication.
(13) International Tables for X-ray Crystallography; Kynoch: Birmingham, England, 1974; Vol. IV.
(14) Cromer, D. T.; Libermann, D. *J. Chem. Phys.* **1970**, *53*, 1981.
(15) Sheldrick, G. M. "SHELX 76 Computing System of Crystallography Programs"; University of Cambridge, Cambridge, England, 1976.

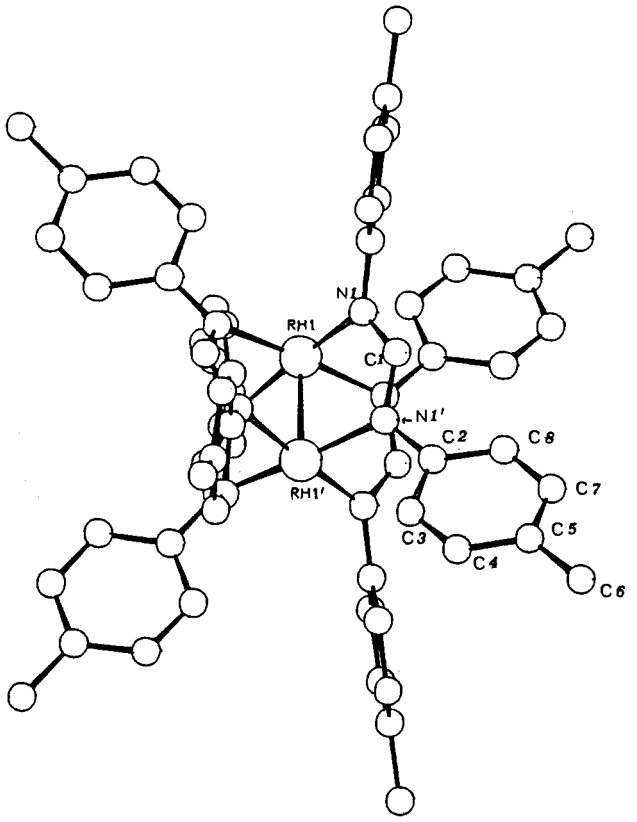

Figure 1. Molecular structure of $Rh_2(form)_4$ with atomic labels.

can be reconverted to the starting complex by heating at 100 °C for 2 h. The ^{13}C NMR spectrum shows a large upfield shift of the carbonyl resonance which does not fall into the region normally associated with terminal CO in rhodium complexes. The assignment of the ^{13}CO resonance at δ 144.06 was confirmed treating a dichloromethane solution of a decarbonylated sample with ^{13}CO. The ^{13}C NMR spectrum of the pink-red complex $Rh_2(form)_4(^{13}CO)$ [$\nu(^{13}CO)$ 1996 cm^{-1}] has the same characteristics as before but with the signals due to the carbonyl group now predominating. The ^{13}C NMR for the methyl carbon atoms appear as equally intense singlets at 19.82 and 19.68 ppm, indicating that the rhodium nuclei are no longer chemically equivalent.

It is worthwhile mentioning that stable adducts of $Rh_2(carboxylate)_4$ with carbon monoxide have never been isolated (the only structure reported was carried out at −190 °C[16]) because they are unstable relative to CO loss (i.e., the complex $Rh_2(perfluorobutyrate)_4(CO)$ loses CO while in the IR beam[17]). In all the carboxylate derivatives the carbonyl is weakly bonded, as evidenced by the ν(CO) which ranges from 2090 cm^{-1} [in the comlex $Rh_2(form)_2(O_2CCF_3)_2(H_2O)_2$[18]] to 2150 cm^{-1} [in the complex $Rh_2(trifluoroacetate)_4$[19]]. Recently these findings stimulated a controversy concerning the nature of the Rh_2^{4+}–CO bond, particularly the metal π^* to CO π^* back-bonding interaction. Some authors suggested, on the basis of the very high ν(CO) frequencies, that the σ donation from the carbonyl is the main component of Rh–C bond.[19] Results by Drago and coworkers,[17,20] on the other hand, based on calorimetric measurements, were considered to be consistent with a pronounced π back-bonding. The value of 2040 cm^{-1} for ν(CO) in **2** reveals significant transfer of π-electron density from the Rh_2^{4+} core to the π^* orbital of the carbonyl group, and certainly this result must be ascribed to the presence of four *p*-tolylformamidinate groups, which place more electronic density than the carboxylate groups into the Rh–Rh unit. The present conclusion is in good agreement with the results reported by Bear and Kadish (after this paper was submitted) on the ability of $Rh_2(O_2CCH_3)_n(HNOCCH_3)_{4-n}$ to bind reversibly carbon monoxide.[21]

Table I. Bond Lengths (Å), Interbond Angles (deg), and Relevant Torsion Angles (deg)

Distances			
Rh(1)–Rh(1)′	2.4336 (4)	C(4)–C(5)	1.409 (10)
Rh(1)–N(1)	2.050 (5)	C(5)–C(7)	1.361 (10)
C(1)–N(1)	1.331 (5)	C(7)–C(8)	1.400 (9)
N(1)–C(2)	1.399 (6)	C(8)–C(2)	1.400 (9)
C(2)–C(3)	1.386 (7)	C(5)–C(6)	1.513 (8)
C(3)–C(4)	1.375 (8)		
Angles			
N(1)–Rh(1)–N(1)′	175.4 (2)	N(1)–C(2)–C(8)	112.8 (6)
Rh(1)–Rh(1)′–N(1)	87.7 (2)	C(2)–C(3)–C(4)	119.3 (7)
N(1)–C(1)–N(1)′	123.7 (8)	C(3)–C(4)–C(5)	123.0 (8)
C(2)–N(1)–C(1)	117.7 (6)	C(4)–C(5)–C(6)	123.0 (9)
C(2)–N(1)–Rh(1)	124.3 (4)	C(4)–C(5)–C(7)	117.4 (8)
N(1)–C(2)–C(3)	119.9 (6)	C(6)–C(5)–C(7)	119.6 (9)
C(5)–C(7)–C(8)	120.7 (8)	C(7)–C(8)–C(2)	121.2 (7)
Torsion Angles			
N(1)–Rh(1)–Rh(1)′–N(1)′		−16.7 (2)	
C(1)–N(1)–C(2)–C(3)		139.3 (6)	
Rh(1)–N(1)–C(2)–C(3)		−43.3 (8)	

Table II. Fractional Coordinates (×10^4)

atom	*x/a*	*y/b*	*z/c*
Rh(1)	5000	579.7 (3)	5000
C(1)	4106 (3)	0	4106 (3)
N(1)	4418 (2)	541 (2)	4217 (2)
C(2)	4345 (3)	1036 (3)	3777 (4)
C(3)	4283 (3)	1658 (3)	3990 (3)
C(4)	4196 (4)	2139 (3)	3553 (4)
C(5)	4178 (4)	2032 (4)	2891 (5)
C(6)	4081 (5)	2561 (5)	2410 (5)
C(7)	4263 (5)	1423 (5)	2684 (4)
C(8)	4353 (4)	926 (3)	3119 (4)
H(0)	3751 (5)	0	3751 (5)
H(3)	4297 (6)	1752 (6)	4449 (6)
H(4)	4150 (6)	2578 (6)	3711 (6)
H(61)	4110 (5)	2979 (5)	2615 (5)
H(62)	3659 (5)	2512 (5)	2215 (5)
H(63)	4410 (5)	2526 (5)	2081 (5)
H(7)	4258 (5)	1329 (5)	2225 (5)
H(8)	4425 (6)	492 (6)	2961 (6)

Crystal Structure of $Rh_2(form)_4$ (1). The molecule is shown in Figure 1 together with the atomic numbering scheme. Bond distances, bond angles, and torsion angles are reported in Table I. Final positional parameters are listed in Table II.

The molecular structure of **1** consists of four formamidinate groups symmetrically disposed about the Rh–Rh unit and is basically analogous to that of the carboxylate derivatives. The Rh–Rh bond length of 2.4336 (4) Å lies at the top of the range of distances observed in these complexes. It is longer than that of the very close complex $Rh_2(benzamidinate)_4$ (2.389 Å).[5] It is noteworthy that the carboxylates form complexes in which the M–M distance ranges from 2.091 Å [$Mo_2(O_2CCMe_3)_4$[22]] to 2.88 Å [$Cu_2(O_2CCF_3)_4(Quin)_2$[23]] while in the amidate derivatives the same distance ranges from 1.843 Å [$Cr_2(MeNCPhNMe)_4$[24]] to 2.982 Å ([$Rh_2\{\mu$-$CPh(NPh)_2\}_2(tfbb)_2$][25]). The significant difference of 0.045 Å between the Rh–Rh bond lengths of the complexes $Rh_2(benzamidinate)_4$ and **1** can be ascribed to the steric

(16) Koh, Y. B. Ph.D. Thesis, The Ohio State University, Columbus, OH, 1979.
(17) Drago, R. S.; Long, S. R.; Cosmano, R. *Inorg. Chem.* **1982**, *21*, 2196.
(18) Unpublished results.
(19) Sowa, T.; Kawamura, T.; Shida, T.; Yonezawa, T. *Inorg. Chem.* **1983**, *22*, 56.
(20) Drago, R. S.; Tanner, S. P.; Richman, R. M.; Long, J. R. *J. Am. Chem. Soc.* **1979**, *101*, 2897.
(21) Chavan, M. Y.; Ahsan, M. Q.; Lifsey, R. S.; Bear, J. L.; Kadish, K. M. *Inorg. Chem.* **1986**, *25*, 3218.
(22) Cotton, F. A.; Extine, M.; Gage, L. D. *Inorg. Chem.* **1978**, *17*, 172.
(23) Moreland, J. A.; Doedens, R. J. *J. Am. Chem. Soc.* **1975**, *97*, 508.
(24) Bino, A.; Cotton, F. A.; Kaim, W. *Inorg. Chem.* **1979**, *18*, 3566.
(25) Lahoz, F. J.; Tiripicchio, A.; Camellini Tiripicchio, M.; Oro, L. A.; Pinillos, M. T. *J. Chem. Soc., Dalton Trans* **1985**, 1487.

hindrance of the phenyl groups attached to the central carbon atom of the benzamidine. The N–C–N angle of the formamidinate groups [123.7 (2)°] is comparable with the values found in the complexes $Rh_2(form)_3(NO_3)_2$[9] and $Rh_2(form)_2(O_2CCF_3)_2(H_2O)_2$, but it is larger than those observed in Mo, Re, and Cr benzamidinate complexes[1] and in the binuclear Rh[1] complex $[Rh_2\{\mu\text{-}CPh(NPh)_2\}_2(tfbb)_2]$.[25]

The rhodium atoms are displaced 0.082 Å out of the least-squares plane determined by each group of four equivalent nitrogen donor atoms. This displacement of metals is toward the axial sites, which are free of ligands in the crystalline state. Nonbonding contacts force the *p*-tolyl groups to rotate out of the plane defined by the N–C–N fragments by 40.07°, leading to an energetically unfavorable reduction of the formamidine π conjugation, and press the molecule to the staggered conformation with the N–Rh–Rh–N torsion angle [16.7 (2)°] similar to that found in the complex $Rh_2(benzamidinate)_4$.[5]

In the title complex the presence of the *p*-tolyl groups on the nitrogen donor atoms makes axial coordination unfavorable even by a hypothetical water molecule. For such an axially coordinated group at an Rh–O bond distance of about 2.36 Å, there are close contacts with H(3) attached to C(3), leading to an O_{water}–C(3) separation of 2.86 Å. The Rh–N bond distances of 2.050 (5) Å are equal to the values found in the compound $Rh_2(benzamidine)_4$, are in agreement with the values reported for $Rh_2(form)_3(NO_3)_2$ [2.033 (10)[9]], though in the latter the metal atoms are in the 2.5 formal oxidation state and the Rh–Rh separation is 0.051 Å longer than that found in the present compound, and are longer than those found in the complex $Rh_2(form)_2(O_2CCF_3)_2(H_2O)_2$ [1.993 (4) Å[10]], where the nitrogen donor atoms are trans to the oxygen atoms of the trifluoroacetate groups. Within the N–C–N fragment the N(1)···N(1)′ separations are 2.346 (5) Å and the N–C [1.331 (5) Å] and the N–C(*p*-tolyl) bond lengths [1.339 (6) Å] are in the range of lengths quoted for N–C bonds of orders 1.5 and 1.0, respectively, as expected for nitrogen and carbon atoms sp^2 hybridized.

Electrochemistry. The cyclic voltammogram recorded at a platinum electrode on a CH_2Cl_2 solution of **1** displays two well-shaped anodic processes as well as one cathodic process, each one of these steps showing a directly associated response in the reverse scan (Figure 6, deposited as supplementary material). Controlled-potential coulometric tests performed in correspondence to the first anodic process indicated the consumption of 1 mol of electrons/mol of starting complex. On the basis of the relative peak heights, both the second anodic process and the cathodic one involve one-electron charge transfers too on the cyclic voltammetric time scale.

As in the case of other dirhodium(II) complexes,[4,5,7,10] we attribute the two anodic steps to the Rh(II)–Rh(II)/Rh(II)–Rh(III) and Rh(II)–Rh(III)/Rh(III)–Rh(III) successive charge transfers, respectively.

The analysis of the cyclic voltammetric responses relevant to the first anodic process with scan rate varying from 0.02 to 50 V s^{-1} showed the following features: the i_{pc}/i_{pa} ratio is constantly equal to unity; the current function $i_{pa}/v^{1/2}$ remains constant; the ΔE_p value gradually increases from 68 mV at 0.02 V s^{-1} to 470 mV at 50 V s^{-1}. All these data are diagnostic for a simple one-electron quasi-reversible charge transfer.

In the course of the controlled-potential one-electron oxidation at the first anodic process (working potential +0.5 V), the solution turns from green to red. The resulting red mixed-valent product Rh(II)–Rh(III) was examined by ESR spectroscopy. Figure 2 shows the relevant spectra recorded in dichloromethane solution at both room (a) and liquid-nitrogen (b) temperature. The sharp single line absorption (line width 25.0 G) obtained at room temperature is characteristic of a paramagnetic species with structural anisotropies ($g_\perp$, $g_\parallel$, $A_\perp$, $A_\parallel$) completely averaged (fast molecular motion conditions). The spectrum at 100 K shows two absorption lines; the low-field one is unresolved, while the high-field one is split into a triplet. These findings can be easy interpreted on the basis of a magnetic interaction between one electron and two ^{103}Rh nuclei ($I = {}^1/_2$).[7a]

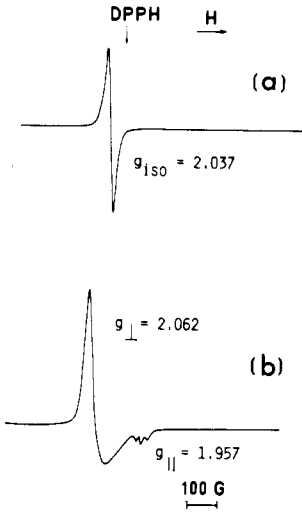

Figure 2. ESR spectra of the electrochemically generated monocation $[Rh_2(form)_4]^+$ recorded in CH_2Cl_2–$[NBu_4]ClO_4$ (0.1 mol dm^{-3}): (a) 300 K; (b) 100 K.

The ESR spectrum in frozen solution is indicative of a paramagnetic system formed by two equivalent Rh nuclei and one delocalized electron in axial symmetry. In fact the high-field pattern displays a resolved hyperfine structure, with 1:2:1 relative intensities, as expected for the aIS (hyperfine term) in the Hamiltonian of the Rh–Rh system. The unresolved hyperfine structure of the low-field line absorption does not allow us the evaluation of $A_\perp$ in the absence of computer fitting simulation. On the contrary, the $g_\parallel$ = 1.957 absorption allows the computation of $A_\parallel = 18.9 \times 10^{-4}$ cm^{-1}.

For the second anodic process, the analysis of the relevant cyclic voltammetric responses with the scan rate reveals the features typical of a quasi-reversible charge transfer followed by a slow chemical reaction involving the electrogenerated species Rh(II–I)–Rh(III). This conclusion is also supported by controlled-potential coulometric tests coupled to ESR measurements. In fact, after the consumption of 2 electrons/molecule (working potential +1.15 V), even if the cyclic voltammogram reveals the presence of the dirhodium(III) species, the electrolysis current falls but still remains significantly higher than the background current. We have not followed the coulometric experiment any longer, since in the analogous process for $Rh_2(form)_2(O_2CCF_3)_2{\cdot}2H_2O$ more than 5 electrons/molecule was slowly consumed.[10] However ESR tests gave sufficient information about the overall anodic process. Just after the consumption of 2.3 electrons/molecule, the electrogenerated deep blue solution shows the presence of about one-tenth of a paramagnetic Rh(II)–Rh(III) species, with respect to the same solution electrolyzed at the first anodic process. In addition, in the blue sample, stored at +5 °C in the ESR tube, a pink-red color is gradually restored primarily at the bottom of the tube (i.e., out of the contact of air), and the amount of paramagnetic Rh(II)–Rh(III) species (g_{iso} = 2.037) increases with time. After about 80 h the Rh(II)–Rh(III) mixed-valent species is almost completely regenerated. All these data can be accounted for by at least two likely, concomitant or alternative, pathways: (i) a solvent-mediated self-reduction process; (ii) considering that formamidine is a noninnocent ligand (free *p*-tolylformamidine is irreversibly oxidized in CH_2Cl_2–$[NBu_4]ClO_4$ (0.1 mol dm^{-3}) solution at +1.1 V), an intramolecular oxidation of the formamidine ligand by the electrogenerated Rh(III)–Rh(III) moiety, which regenerates the mixed-valent species, but with some peripheral modification of the ligand.

This could constitute a general explanation of the instability of dirhodium(III) dimers with acetamidate and phenylacetamidate ligands[7] and with formamidinate and trifluoroacetate ligands.[10]

An interesting feature of the redox chemistry of the here presented tetrakis(formamidinato) complex is the appearance, in cyclic voltammetry, of a well-formed one-electron cathodic process, showing a directly associated reoxidation response.

Table III. Formal Electrode Potentials (in Volts, vs. SCE) for Redox Changes of Dirhodium Complexes in CH_2Cl_2 Solution and Relevant Comproportionation Constants for Stabilization of Rh(II)–Rh(III) Mixed-Valent Species

complex	$E^{\circ\prime}$ Rh(III)–Rh(III)/ Rh(III)–Rh(II)	$E^{\circ\prime}$ Rh(III)–Rh(II)/ Rh(II)–Rh(II)	K_{com}(Rh(III)–Rh(II))	$E^{\circ\prime}$ Rh(II)–Rh(II)/ Rh(II)–Rh(I)	ref
$Rh_2(O_2CCF_3)_4$		~+1.8			7a
$Rh_2(O_2CC_3H_9)_4$		+1.59			20
$Rh_2(ONHCCF_3)_4$		~+1.1			7a
$Rh_2(C_6H_5NOCCH_3)_4$	+1.65	+0.55	4×10^{18}		7a
$Rh_2(form)_2(O_2CCF_3)_2(H_2O)_2$[a]	+1.44	+0.76	3×10^{11}	−1.25[c]	10
$Rh_2(form)_4$[a]	+1.06	+0.25	5×10^{13}	−1.33	this work
$Rh_2(benzam)_4$[b]	+1.24	+0.23	1×10^{17}	−1.58	5
$Rh_2(PhNpy)_4$	+0.60	−0.05	1×10^{11}	−1.1[c]	4
$Rh_2(3,5\text{-}Me_2pz)_4$		+1.1[c]			6

[a] form = *N,N'*-di-*p*-tolylformamidinato. [b] benzam = *N,N'*-diphenylbenzamidinato. [c] Peak potential values for irreversible charge transfers.

Table IV. Formal Electrode Potentials (in Volts, vs. Ferrocenium/Ferrocene Couple) for Redox Changes of $Rh_2(form)_4$ in Different Solvents

solvent	$E^{\circ\prime}$ Rh(II)–Rh(II)/Rh(II)–Rh(III)	ΔE_p[b]	$E^{\circ\prime}$ Rh(II)–Rh(III)/Rh(III)–Rh(III)	ΔE_p[b]	$E^{\circ\prime}$ Rh(II)–Rh(II)/Rh(II)–Rh(I)	ΔE_p[b]
CH_2Cl_2	−0.23	90	+0.58	94	−1.81	100
MeCN[a]	−0.36	64	+0.48	66	−1.76	120
THF	−0.24	140			−1.85	140
DMF	−0.40	68	+0.36	90	−1.69	120
py	−0.39	110			−1.75	120

[a] The dirhodium(II) complex is very slightly soluble. [b] Measured at a platinum electrode at 0.2 V s^{-1}.

As it happens for $Rh_2(form)_2(O_2CCF_3)_2$ (Figure 6), most of the electroreducible dirhodium(II) complexes involve totally irreversible charge transfers.[26-28] Some mixed carboxylate-substituted 1,8-naphthyridine complexes[29a,b] display multiple one-electron reversible reductions, but they are likely centered on the aromatic ligand[29a,c] and do not involve the dirhodium(II) moiety. Only in the case of the recently reported tetrakis(benzamidinato) complex $Rh_2(N_2Ph_2CPh)_4$,[5] closely related to the present compound, has there been observed a reversible change transfer leading to the mixed-valent Rh(II)–Rh(I) species.

The analysis of the cyclic voltammetric responses relevant to the cathodic process with the scan rate shows that the directly associated reoxidation peak is practically absent at 0.02 V s^{-1}, gradually increasing until at 2 V s^{-1} the anodic to cathodic peak current ratio reaches unity, and that the ΔE_p term gradually increases from 86 mV at 0.05 V s^{-1} to 450 mV at 50 V s^{-1}. These data must be interpreted in terms of a one-electron quasi-reversible charge transfer complicated by following chemical reactions. The use of scan rates higher than 2 V s^{-1} allows us however to prevent the chemical complications following the charge transfer and hence to compute a formal electrode potential for the one-electron cathodic process Rh(II)–Rh(II)/Rh(II)–Rh(I). In addition, assuming a first-order chemical reaction to follow the cathodic step, we can roughly evaluate, with the appropriate working curve of Nicholson,[30] a half-life of about 5 s for the Rh(II)–Rh(I) congener.

Controlled-potential coulometric tests performed at the potentials of the reduction process (working potential −1.4 V) showed however that on the longer time scale this cathodic process involves a multielectron charge transfer. Since, on the basis of the cyclic voltammograms recorded after the bulk electrolysis, in this process a stable species somewhat different from the starting one is likely generated, further investigations are needed for its complete characterization.

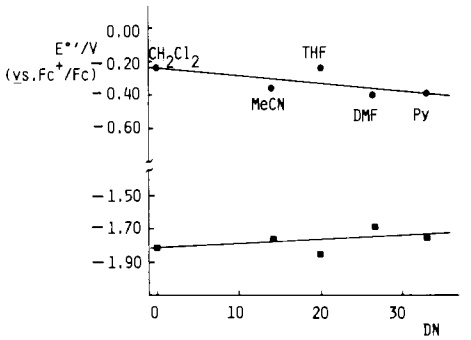

Figure 3. Dependence of the formal electrode potentials of the couples Rh(II)–Rh(II)/Rh(II)–Rh(III) (●) and Rh(II)–Rh(II)/Rh(II)–Rh(I) (■) on the solvent donor number.

In conclusion, some significant differences hold with respect to the electrochemical behavior of tetrakis(benzamidinato)dirhodium(II); in particular, Bear and Kadish[5] have found that this latter compound undergoes a one-electron quasi-reversible cathodic reduction, which generates the corresponding Rh(II)–Rh(I) species, stable under anaerobic conditions.

Table III summarizes the standard electrode potentials for the redox changes observed for **1**, together with those for other tetrasubstituted dirhodium complexes, which confirm that in most cases eight-nitrogen coordinations thermodynamically favor the sequential oxidations of dirhodium(II) dimers. Also reported are the relevant comproportionation constants, K_{com}, calculated according to Gagné's method,[31] for the equilibrium

$$\text{Rh(II)–Rh(II)} + \text{Rh(III)–Rh(III)} \overset{K_{com}}{\rightleftharpoons} 2\text{Rh(II)–Rh(III)}$$

which reflect the extent of the thermodynamic stabilization of the mixed-valent species Rh(II)–Rh(III). We point out here that according to Gagné the present complex, having a K_{com} of 5×10^{13}, must be classified as a class III Robin–Day[32] mixed-valent species (i.e., completely delocalized). Even if, in some cases, such computations have been criticized,[33] we note that low-temperature ESR tests confirm that in the present case the electron is delo-

(26) Das, K.; Kadish, K. M.; Bear, J. L. *Inorg. Chem.* **1978**, *17*, 930 and references therein.
(27) Chakravarty, A. R.; Cotton, F. A.; Tocher, D. A.; Tocher, J. H. *Organometallics* **1985**, *4*, 8.
(28) Kadish, K. M.; Lancon, D.; Dennis, A. M.; Bear, J. L. *Inorg. Chem.* **1982**, *21*, 2987 and references therein.
(29) (a) Tikkanen, W. R.; Binamira-Soriaga, E.; Kasha, W. C.; Ford, P. C. *Inorg. Chem.* **1984**, *23*, 141. (b) Thummel, R. P.; Lefoulon, F.; Williamson, D.; Chavan, M. *Inorg. Chem.* **1986**, *25*, 1675. (c) Bear, J. L.; Chau, L. K.; Chavan, M. Y.; Lefoulon, F.; Thummel, R. P.; Kadish, K. M. *Inorg. Chem.* **1986**, *25*, 1514.
(30) Nicholson, R. S.; Shain, I. *Anal. Chem.* **1964**, *36*, 706.
(31) Gagné, R. R.; Spiro, C. L.; Smith, T. J.; Hamann, C. A.; Thies, W. R.; Shiemke, A. K. *J. Am. Chem. Soc.* **1981**, *103*, 4073.
(32) Robin, M. B.; Day, P. *Adv. Inorg. Chem. Radiochem.* **1967**, *10*, 247.
(33) Drago, R. S.; Desmond, M. J.; Corden, B. B.; Miller, K. A. *J. Am. Chem. Soc.* **1983**, *105*, 2287.

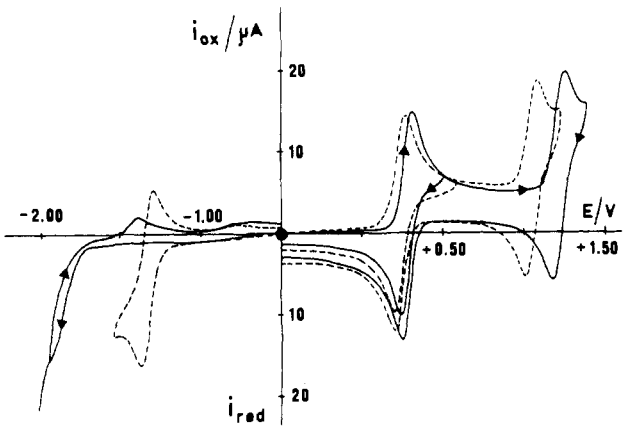

Figure 4. Cyclic voltammograms obtained at a platinum electrode in a CH_2Cl_2 solution containing $Rh_2(form)_4$ (1.0×10^{-3} mol dm^{-3}) and $[NBu_4]ClO_4$ (0.1 mol dm^{-3}) under the following experimental conditions: (---) deaerated; (—) saturated with CO. Scan rate: 0.2 V s^{-1}.

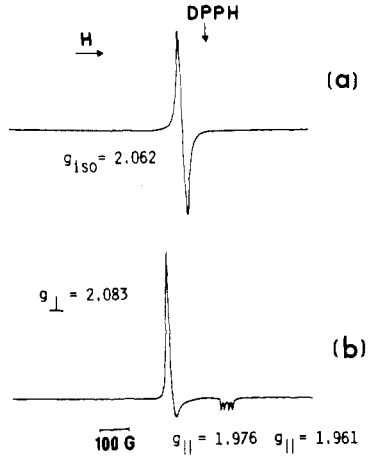

Figure 5. ESR spectra recorded on a CH_2Cl_2 solution of $Rh_2(form)_4$ (containing $[NBu_4]ClO_4$ (0.1 mol dm^{-3})) exhaustively one-electron-oxidized at +0.5 V under CO atmosphere: (a) room temperature; (b) 100 K.

calized over both the rhodium centers. The same complete delocalization on the ESR time scale has been also observed for both the tetrakis(benzamidinato) complex[5] and the tetrakis(phenylacetamidato) complex,[7] which display large K_{com} values.

Even though **1** is only slightly soluble in many solvents, we have tested its electrochemical behavior in a few nonaqueous media. Table IV reports the formal electrode potentials computed in these solvents for the above mentioned redox changes; in order to correct for variable liquid junction potentials, the ferrocenium/ferrocene couple was used as an internal reference. Also reported are the differences, ΔE_p, between a forward peak potential value and the peak potential value of the directly associated response, which measure the extent of reversibility of a charge transfer, when compared with the theoretical value of 59 mV for a reversible one-electron step. These values clearly show that in most cases the charge transfers are quasi-reversible in character. Figure 3 shows a plot of the formal electrode potentials of both Rh(II)–Rh(II)/Rh(II)–Rh(III) and Rh(II)–Rh(II)/Rh(II)–Rh(I) redox changes as a function of the Gutmann donor number.[34] Linear regression analysis for the two straight lines gives correlation coefficients of −0.72 for the one-electron oxidation and 0.49 for the one-electron reduction. These values denote that the donor number is insufficient to fully account for solvent effect–redox potential relationships, and we shall present elsewhere a more complete approach to this topic through multiparameter equations;[35] notwithstanding, this plot shows that, as expected,[7,10,26] coordinating solvents make easy the access to the one-electron oxidized dimer, destabilizing its HOMO level through an axial binding. However, in agreement with the chemical evidence for a very low tendency toward axial coordination of the complex presented here, this destabilization is much more attenuated with respect to that occurring for tetracarboxylates[26] and tetraamidates,[7] as pointed out from the slope values of the relevant straight lines [−0.011 for $Rh_2(ONHCCF_3)_4$, $Rh_2(O_2CC_2H_5)_4$, and $Rh_2(C_6H_5NOCCH_3)_4$; −0.0047 for $Rh_2(form)_4$)]. As regards the Rh(II)–Rh(II)/Rh(II)–Rh(I) reduction, it seems on the contrary that axial binding from solvents slightly stabilizes the LUMO level of the complex, even if the slope of 0.0024 confirms that the σ^* Rh–Rh LUMO has a very weak contribution σ^* from Rh–axial ligands.[5] In this connection, if one considers that thermodynamic redox potentials are directly related to the relative energies of the HOMO/LUMO levels,[36] we can attempt an approximate estimate of the difference in energy between the HOMO and LUMO levels of **1** using the potential values for the couples Rh(II)–Rh(II)/Rh(III)–Rh(II) and Rh(II)–Rh(II)/Rh(II)–Rh(I), in view of the tested low contribution of solvation terms to orbital energies; this difference is of about 1.5 eV.

Electrochemical Behavior of $Rh_2(form)_4$ in the Presence of CO. Figure 4 illustrates the cyclic voltammetric response of **1** in deaerated CH_2Cl_2 solution (dashed line), with respect to that from the same solution saturated with CO (solid line). As a consequence of the presence of CO, the two anodic processes are shifted toward more positive potentials, the second step being involved to an extent greater than the first one. On the contrary, the cathodic process is shifted toward negative potentials very close to that of the solvent discharge, followed clearly by significant changes in the molecular framework.

The analysis of cyclic voltammograms indicates that, under CO, the anodic processes maintain the same electrode characteristics as in absence of CO. In addition, there is no evidence for additional complications following these charge transfers (e.g., decomplexation of the CO molecule). We have carried out a controlled-potential electrolysis at the potentials of the first anodic process under a CO atmosphere, and the resulting deep red-violet solution has been examined by ESR spectroscopy. Figure 5 shows the relevant spectra. The frozen-glass low-field absorption does not show superhyperfine splitting, thus allowing us to disregard the occurrence of gross structural modifications leading to the interaction of nitrogen atoms with the paramagnetic Rh centers. In addition, the high-field absorption exhibits a well-separated doublet of doublets, centered at $g_{||} = 1.976$ ($A_{||} = 10.0 \times 10^{-4}$ cm^{-1}) and at $g_{||} = 1.961$ ($A_{||} = 12.5 \times 10^{-4}$ cm^{-1}), respectively, with a separation of 16.2 G. The room-temperature g_{iso} is equal to 2.062. All these ESR parameters, significantly different from those computed for $[1]^+$, are indicative of the presence of two nonequivalent rhodium nuclei. This behavior is quite reminiscent of the formation of the monoligated CH_3CN adduct of the tetrakis(benzamidinato) complex $[Rh_2(N_2Ph_2CPh_2)_4]^+$.[5]

Hence, considering the likely equilibria

$$Rh^{II}Rh^{II}(form)_4 + CO \overset{K_1}{\rightleftharpoons} Rh^{II}Rh^{II}(form)_4(CO)$$

$$[Rh^{II}Rh^{III}(form)_4]^+ + CO \overset{K_2}{\rightleftharpoons} [Rh^{II}Rh^{III}(form)_4(CO)]^+$$

$$[Rh^{III}Rh^{III}(form)_4]^{2+} + CO \overset{K_3}{\rightleftharpoons} [Rh^{III}Rh^{III}(form)_4(CO)]^{2+}$$

one can estimate the relationships among K_1, K_2, and K_3 by the well-known equation for one-electron steps leading to the reduced form of complexes having the same number of ligands.[37]

$$E^{\circ\prime}_{complex} - E^{\circ\prime}_{free} = \frac{RT}{F} \ln \frac{K_{red}}{K_{ox}}$$

(34) Mayer, U. *Coord. Chem. Rev.* **1976**, *21*, 159.
(35) Seeber, B.; Zanello, P.; Piraino, P., manuscript in preparation.
(36) Saeva, F. D.; Olin, G. R. *J. Am. Chem. Soc.* **1980**, *102*, 299.
(37) Heyrovsky, J.; Kuta, J. *Principles of Polarography*; Academic: New York, 1966; p 156.

in which it has been simplified that diffusion coefficients remain constant in the course of redox processes. On the basis of the anodic shifts of the first and second processes ($\Delta E_1 = 0.04$ V and $\Delta E_2 = 0.17$ V), we obtain $K_1 \simeq 5K_2$ and $K_2 \simeq 8 \times 10^2 K_3$. These results, although roughly computed, are in agreement with the view that oxidation processes remove electrons able to be involved in stabilizing π back-donation toward CO.[20,21] It seems noteworthy that the loss of the two electrons from the HOMO level causes that $K_3 \simeq 2.5 \times 10^{-4} K_1$.

Acknowledgment. We thank the Italian Ministry of Education for financial support. We also thank Professor F. A. Cotton for making the results cited in ref 12 available to us.

Registry No. 1^{2+}, 108149-50-4; 1^{+}, 108149-51-5; **1**, 108149-48-0; 1^{-}, 108149-52-6; **2**, 108149-49-1; $Rh_2(form)_2(O_2CCF_3)_2(H_2O)_2$, 105164-41-8; Rh, 7440-16-6; CO, 630-08-0.

Supplementary Material Available: Cyclic voltammograms of **1** and $Rh_2(form)_2(O_2CCF_3)_2(H_2O)_2$ in CH_2Cl_2 solvent (Figure 6) and a list of temperature factors (Table V) (2 pages); a listing of calculated and observed structure factors (4 pages). Ordering information is given on any current masthead page.

Contribution from the Department of Chemistry and Biochemistry, James Cook University of North Queensland, Townsville, Queensland 4811, Australia, and Department of Chemistry, Brookhaven National Laboratory, Upton, New York 11973

Mode of Coordination of Tris(2-pyridyl)methanol to Ruthenium(II): Synthetic, Spectral, and Structural Studies of the Bis(ligand) Species

F. Richard Keene,*[1] David J. Szalda,*[2] and Tracy A. Wilson[1]

Received September 4, 1986

Two forms of the cation bis[tris(2-pyridyl)methanol]ruthenium(II) have been isolated—a yellow species, $[Ru((py)_3COH)_2]^{2+}$ (**2**), and an orange form in which one ligand is deprotonated, $[Ru((py)_3COH)((py)_3CO^-)]^+$ (**1**). The pK_a for the ligand deprotonation is 3.78 (±0.02) in aqueous 0.1 M KNO_3 at 25.0 °C. X-ray structural determinations show coordination occurs in an (N,N′,N″)(N,N′,O) mode for both complexes, with the coordinated oxygen atom being the site of the acid/base reactivity. The deprotonated species (**1**) has a plane of symmetry with Ru–N bond lengths in the range 2.040–2.063 Å. The nondeprotonated form (**2**) has Ru–N bond lengths in the range 2.046–2.058 Å, except for an abnormally short Ru–N bond (2.023 (2) Å) trans to the coordinated Ru–OH. Additionally, in **2** the plane of symmetry is lost. In aqueous solution the redox potentials for the Ru(III)/Ru(II) couples are 0.40 (**2**) and 0.25 V (**1**) vs. SSCE. The electronic and ^{13}C NMR spectra are also reported. Crystals of the deprotonated form, $[Ru((py)_3COH)((py)_3CO)]Br \cdot 2C_2H_5OH$ (**1a**), are monoclinic, space group $P2_1/m$, with $a = 8.096$ (2) Å, $b = 13.584$ (2) Å, $c = 15.204$ (2) Å, $\beta = 101.96$ (1)°, $V = 1635$ (1) Å^3, and $Z = 2$. Crystals of $[Ru((py)_3COH)_2](CH_3SO_4)_2$ (**2a**) are triclinic, space group $P\bar{1}$, with $a = 13.517$ (3) Å, $b = 14.458$ (2) Å, $c = 9.727$ (2) Å, $\alpha = 104.72$ (2)°, $\beta = 108.56$ (2)°, $\gamma = 92.41$ (2)°, $V = 1727$ (3) Å^3, and $Z = 2$.

Introduction

The ligation of a number of tripodal π-acceptor tridentates to a variety of metal centers has been reported. Canty et al.[3-6] have used a wide range of ligands XY_3 (X = CH, COH; Y = 2-pyridyl, 1-pyrazolyl, *N*-methylimidazol-2-yl) to impose unusual coordination geometries on metal centers such as Hg(II) and Au(III). White and Faller[7] and Szalda and Keene[8] have isolated complexes of cobalt with tris(2-pyridyl)methanol and tris(2-pyridyl)methane, and Boggess and co-workers[9-11] have reported studies of a number of complexes of first-row transition metals with ligands of the type $(2\text{-py})_3X$ (X = N, P, As, P=O, CH, COH). The zinc complexes of the trisubstituted methanols have also been noted[12] as models for the enzyme carbonic anhydrase.

Tris(2-pyridyl)methanol has been shown to be ambiguous with regard to its mode of coordination, with ligation occurring via three py N atoms (N,N′,N″), structure A, or via two py N atoms and the deprotonated alcohol O (N,N′,O$^-$), structure B. For the

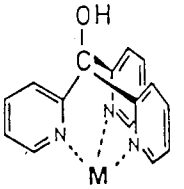

$(py)_3COH$-*N,N′,N″*
A

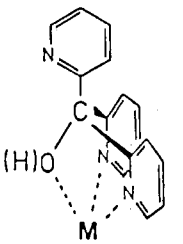

$(py)_3CO(H)$-*N,N′,O*
B

bis(ligand)cobalt(III) species, two linkage isomers were isolated:[8] viz. the symmetrical bis(N,N′,N″) form and the (N,N′,N″)-(N,N′,O$^-$) species. As part of our current general study of complexes of tripodal π-acceptor ligands with metals in Groups 8–10, we now report synthetic and structural studies of the corresponding bis(ligand)ruthenium(II) complex, which have realized only the unsymmetric (N,N′,N″)(N,N′,O$^-$) form and its nondeprotonated analogue (N,N′,N″)(N,N′,O).

Experimental Section

Physical Measurements. Electronic spectra were recorded on a Cary 219 spectrophotometer, and NMR spectra were recorded with a Bruker AM-300 spectrometer (Me_2SO-d_6 solution; Me_4Si reference).

Electrochemical measurements were made by using a Bioanalytical Systems (BAS) CV-27 voltammograph, with cyclic voltammograms

(1) James Cook University of North Queensland.
(2) Brookhaven National Laboratory. Permanent address: Baruch College, New York, NY 10010.
(3) Canty, A. J.; Chaichit, N.; Gatehouse, B. M.; George, E. E.; Hayhurst, G. *Inorg. Chem.* **1981**, *20*, 2414–2422.
(4) Canty, A. J.; Chaichit, N.; Gatehouse, G. M.; George, E. E. *Inorg. Chem.* **1981**, *20*, 4293–4300.
(5) Canty, A. J.; Minchin, N. J.; Healy, P. C.; White, A. H. *J. Chem. Soc., Dalton Trans.* **1982**, 1795–1802.
(6) Canty, A. J.; Patrick, J. M.; White, A. H. *Inorg. Chem.* **1984**, *23*, 3827–3830.
(7) White, D. L.; Faller, J. W. *Inorg. Chem.* **1982**, *21*, 3119–3122.
(8) Szalda, D. J.; Keene, F. R. *Inorg. Chem.* **1986**, *25*, 2795–2799.
(9) Boggess, R. K.; Zatko, D. A. *Inorg. Chem.* **1976**, *15*, 626–630.
(10) Boggess, R. K.; Boberg, S. J. *J. Inorg. Nucl. Chem.* **1980**, *42*, 21–26.
(11) Boggess, R. K.; Hughes, J. W.; Chew, C. W.; Kemper, J. J. *J. Inorg. Nucl. Chem.* **1981**, *43*, 939–945.
(12) Brown, R. S.; Huguet, J. *Can. J. Chem.* **1980**, *58*, 889–901.

0020-1669/87/1326-2211$01.50/0